Geophysical Research Letters

RESEARCH LETTER
10.1029/2024GL112730

Special Collection:
Space Weather Events of 2024 May 9-15

Near-Earth Reconnection Contributing to Recovery Phase of Geomagnetic Storm

Terry Z. Liu[1], Vassilis Angelopoulos[1], Yukitoshi Nishimura[2], Yangyang Shen[1], Xueling Shi[3,4], and Michael D. Hartinger[1,5]

[1]Department of Earth, Planetary, and Space Sciences, University of California, Los Angeles, Los Angeles, CA, USA, [2]Department of Electrical and Computer Engineering and Center for Space Physics, Boston University, Boston, MA, USA, [3]Department of Electrical and Computer Engineering, Virginia Tech, Blacksburg, VA, USA, [4]High Altitude Observatory, National Center for Atmospheric Research, Boulder, CO, USA, [5]Space Science Institute, Boulder, CO, USA

Key Points:

- During the recovery phase of the May 2024 major storm, near-Earth reconnection was likely close enough to contribute to the ring current
- Dipolarizing flux bundles penetrated to ~6.6R_E at midnight with current wedges, auroral brightening, and ionospheric currents identified
- The driver was likely a large dynamic pressure that strongly compressed the magnetosphere, causing an extremely thin current sheet at ~6.6R_E

Supporting Information:

Supporting Information may be found in the online version of this article.

Correspondence to:

T. Z. Liu,
terryliuzixu@ucla.edu

Citation:

Liu, T. Z., Angelopoulos, V., Nishimura, Y., Shen, Y., Shi, X., & Hartinger, M. D. (2024). Near-earth reconnection contributing to recovery phase of geomagnetic storm. *Geophysical Research Letters*, *51*, e2024GL112730. https://doi.org/10.1029/2024GL112730

Received 25 SEP 2024
Accepted 28 NOV 2024

Author Contributions:

Conceptualization: Terry Z. Liu, Vassilis Angelopoulos
Data curation: Terry Z. Liu, Yukitoshi Nishimura, Yangyang Shen
Formal analysis: Terry Z. Liu, Vassilis Angelopoulos, Yukitoshi Nishimura
Investigation: Terry Z. Liu, Vassilis Angelopoulos, Yukitoshi Nishimura, Yangyang Shen, Xueling Shi, Michael D. Hartinger

Abstract Recent observations show very near-Earth reconnection (~8–13R_E) could efficiently power the ring current during the main phase of geomagnetic storms, but whether the recovery phase might be contributed remains unclear. During the recovery phase of the May 2024 major geomagnetic storm, intense auroral brightening and geomagnetic disturbances were observed at midnight, indicative of particle injections. Current wedges observed by mid-latitude ground magnetometers around midnight suggest dipolarizing flux bundles (DFBs). The latitude of the auroral brightening was clearly lower than usual, suggesting near-Earth reconnection (NERX) was closer to Earth than during substorms (~20–30R_E). GOES-18 at midnight detected magnetic field and plasma signatures consistent with DFBs, following an extremely thin current sheet likely compressed by strong upstream dynamic pressure. These results indicate NERX could have been close enough for resultant DFBs to penetrate geosynchronous orbit and contribute to the ring current during the recovery phase. This scenario deserves further examination in future.

Plain Language Summary When a coronal mass ejection hits Earth's magnetic field, significant disturbances in the near-Earth space environment occur, namely geomagnetic storms, causing many hazards to our power systems and space missions. It is thus important to understand the underlying processes, especially how energetic particles are transported from the nightside to energize these disturbances. Nightside magnetic reconnection, which converts magnetic energy to particle energy, was not widely considered as an efficient contributor because it typically occurs too far from Earth. However, by identifying observational characteristics using ground and spacecraft measurements, we find that such magnetic reconnection could be sufficiently close to Earth to transport energy and particles to geosynchronous orbit during the recovery phase of a geomagnetic storm. Our results improve our understanding of energy transport during the recovery phase, which will help understand and mitigate space weather hazards in the future.

1. Introduction

Geomagnetic storms (e.g., Gonzalez et al., 1994) are a major contributor to space weather hazards, such as disruptions of power systems and communications (e.g., MacAlester & Murtagh, 2014). During storms, solar wind energy is input from the dayside to the magnetotail and back toward the magnetosphere, which energizes the ring current that depletes the low-latitude geomagnetic field as indicated by the Dst or SYM-H indices (e.g., review by Buzulukova et al., 2018). Although the ring current is crucial to storm dynamics, there are ongoing debates about whether the ring current is powered by global circulation driven by dayside magnetopause reconnection (e.g., Dungey, 1961; Gonzalez et al., 1989) or by bursty bulk flows (BBFs) resulting from nightside magnetotail reconnection (Angelopoulos et al., 1992, 1994).

Near-Earth magnetotail reconnection (NERX) typically occurs at X ~ −20 to −30 R_E (e.g., Angelopoulos et al., 2008). Simulations (e.g., Cramer et al., 2017; Sorathia et al., 2021; Yang et al., 2016) have demonstrated that when the resulting BBFs reach geosynchronous orbit, they are an important contributor to the ring current, through associated inductive electric field, potential electric field, and impulsive transport (e.g., Keika et al., 2013). However, because of reconnection's typical distance far downtail, only a small fraction of the BBFs can reach geosynchronous orbit during either non-storm time (Dubyagin et al., 2011; Sergeev et al., 2012) or storm time (Runov et al., 2021). Closer to Earth, on the other hand, the strong dipole fields tend to suppress magnetotail reconnection (Pellat et al., 1991). Thus, although NERX is common during storms, its direct

Methodology: Terry Z. Liu, Vassilis Angelopoulos
Supervision: Vassilis Angelopoulos
Validation: Terry Z. Liu
Visualization: Terry Z. Liu, Yukitoshi Nishimura
Writing – original draft: Terry Z. Liu
Writing – review & editing: Terry Z. Liu, Vassilis Angelopoulos, Yukitoshi Nishimura, Yangyang Shen, Xueling Shi, Michael D. Hartinger

contribution to powering the ring current has been considered inefficient. However, recent observations by Angelopoulos et al. (2020) and Runov et al. (2022) have identified that very near-Earth reconnection (VNERX) can occur at X ∼ −8 to −13 R_E during the main phase, efficiently powering the ring current. Its occurrence is attributed to the intense solar wind dynamic pressure and southward interplanetary magnetic field (IMF), enabling a thin current sheet geometry very near Earth (e.g., Sciola et al., 2023). A recent statistical study by Beyene and Angelopoulos (2024) estimated the occurrence rate of VNERX to be 1.3 events per 1,000 hr of storm main phase observations, and negligible during recovery phase.

Even though during storm recovery phase NERX may not occur earthward of X ∼ −13 R_E (for it to satisfy the operational criteria of a VNERX), it may still occur closer to Earth than during non-storm times, such that it is more geoeffective, and contribute to ring current energization. On 10 May 2024, a coronal mass ejection (CME) triggered a major geomagnetic storm with the Dst and SYM-H indices exceeding −400 and −500 nT, respectively. This storm provides a good opportunity to examine whether such NERX may supply power to the ring current, which could slow down its decay during the recovery phase. Even though there was no monitor of tail flows at 13–20 R_E, we present evidence that NERX could be close enough for dipolarizing flux bundles (DFBs) to penetrate geosynchronous orbit, indicating that its contribution to the ring current during the recovery phase could be more efficient than previously thought. We introduce our data set in Section 2, demonstrate our results in Section 3, and summarize them in Section 4.

2. Data

We utilize the Acceleration, Reconnection, Turbulence and Electrodynamics of the Moon's Interaction with the Sun (ARTEMIS) mission, which was part of the Time History of Events and Macroscale Interactions during Substorms (THEMIS) before 2010 (Angelopoulos, 2008), to monitor solar wind conditions at lunar orbit. Korean Multi-Purpose Satellite (KOMPSAT) magnetometer observations (Kim, 1999; Magnes et al., 2020) and Geostationary Operational Environmental Satellite-R (GOES-R) observations (Goodman et al., 2012) are also used to examine responses in the magnetosphere at geosynchronous orbit. We employ observations from the THEMIS ground magnetometer network (Russell et al., 2009), ground magnetometer networks obtained via the SuperMAG database (Gjerloev, 2012), and international real-time magnetic observatory network database (INTERMAGNET; Kerridge, 2001) as well as white-light images from the THEMIS All-Sky Imager network (ASI; Donovan et al., 2006). We also use vertical total electron content (TEC) maps in North America from GPS (Hofmann-Wellenhof et al., 1998).

3. Results

Figure 1 provides an overview of the geomagnetic storm event on 11 May 2024, when it transitioned from the main phase to the recovery phase, as seen from the SYM-H index (Figure 1e). Within the CME sheath region, the upstream density varied very significantly from ∼10 to 80 cm^{-3} (Figure 1b) and the ion bulk velocity was almost 800 km/s (Figure 1c), leading to very intense dynamic pressure variations (from several to ∼30 nPa in Figure 1d). Such dynamic pressure variations caused considerable compression and expansion of the magnetosphere globally, so variations in the SYM-H index were partially correlated with the dynamic pressure variations (through the magnetopause current).

Corresponding to the dynamic pressure increase and decrease at t1–t4, the substantial back-and-forth motion of the magnetopause caused KOMPSAT on the dayside (green in Figure 1j) to temporarily enter the magnetosheath twice (Figure 1f). GOES-18, initially on the dayside (blue in Figure 1j), also briefly entered the magnetosheath at t1 (Figure 1i). Due to global expansion, GOES-16 around pre-midnight (magenta in Figure 1j) observed a local minimum in B_x with strong B_z at t2 (i.e., more dipole-like) followed by an increase in B_x and a decrease in B_z (i.e., more magnetotail-like) until t3 due to gradual compression. Similarly, local compression at t5 and significant compression at t6 resulted in local increases in the SYM-H index. Meanwhile, GOES-18 around midnight observed increases in B_x and decrease in B_z, while GOES-16 around dawnside observed magnetic field strength enhancements. Notably, after t5 and t6, the AE index exceeded 3,000 nT twice (Figure 1i), prompting a further examination of this time interval.

Figure 2a shows that corresponding to each extreme enhancement in the AE index, intense auroral brightening was observed by the ASI at the Athabasca station (magnetic local time (MLT) was ∼1.4 hr at 09:00 UT). The first

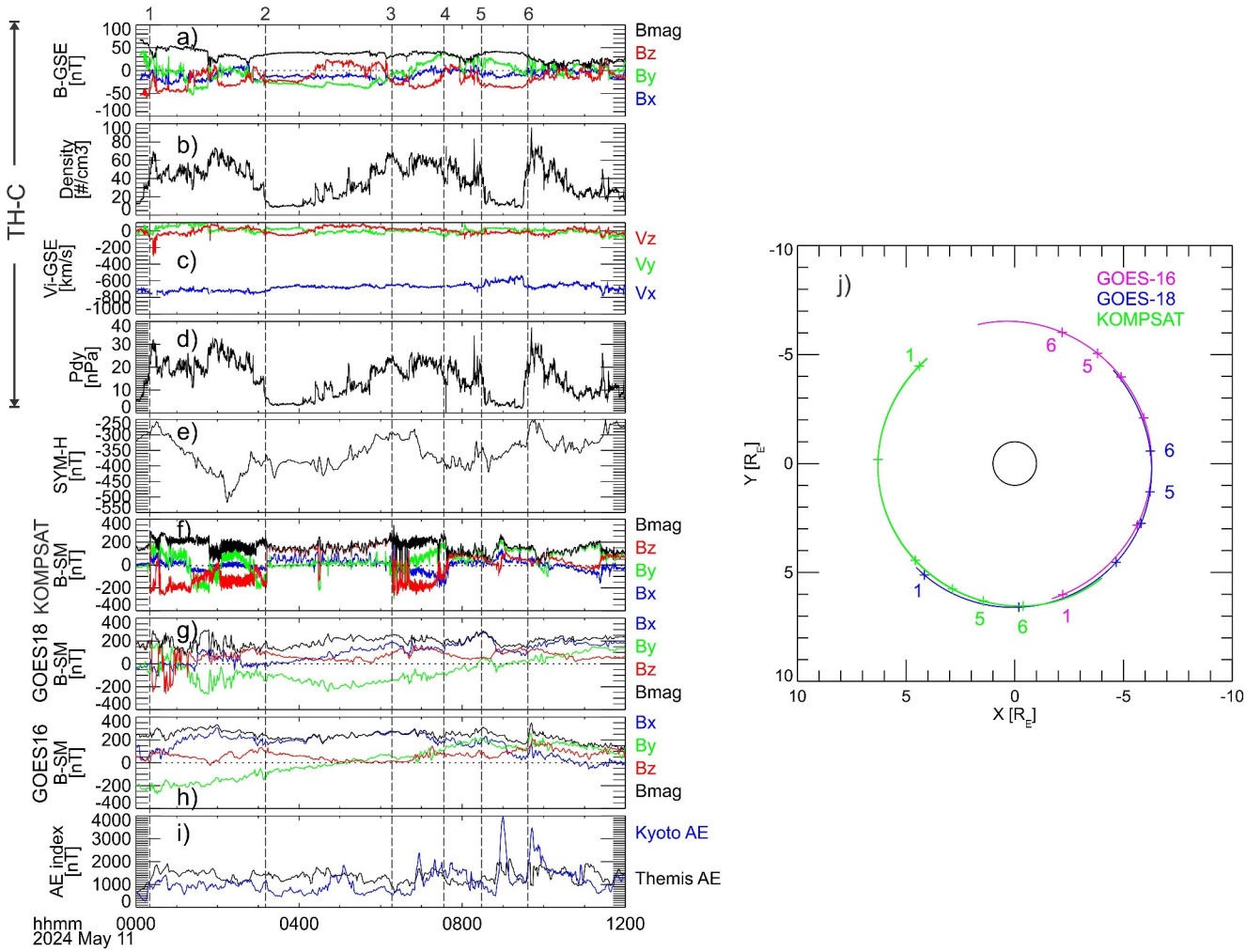

Figure 1. Overview of the event, including TH-C observations of (a) the magnetic field in GSE, (b) electron density, (c) ion bulk velocity in GSE, and (d) dynamic pressure, (e) SYM-H index from OMNI, (f) KOMPSAT observations of the magnetic field in SM, (g) GOES-18 observations of the magnetic field in SM, (h) GOES-16 observations of the magnetic field in SM, (i) AE index from THEMIS and Kyoto, and (j) position of spacecraft at the geosynchronous orbit with numbers indicating time corresponding to vertical dashed lines (t1–t6).

auroral brightening (at ~08:50 UT) expanded poleward from magnetic latitude (MLAT) of at least ~55°–~75° (also see Movie S1). The ASI at the Lucky Lake station, slightly east of Athabasca by ~6°, observed eastward expansion of the auroral brightening (see Movie S2). Several minutes later at ~08:52 UT, the ASI at the Pinawa (PIN) station (MLT of ~2.6 hr), although partly cloudy, observed auroral brightening (see Movie S3). The second brightening (at ~09:40 UT) was diffuse auroral brightening without substorm-like signatures (Figure 2a), so our analysis focuses on the first one. During both brightenings, ground magnetometers at high MLAT observed very significant disturbances around midnight (Figures 2b–2d; much weaker disturbances away from midnight were not shown). Especially during the first brightening, the D-component variations show sign-reversal along MLAT, consistent with current systems typical of deep injections (Yang et al., 2012)—their extremely large magnitude (4,000–6,000 nT) suggests unusually high current intensity. Additionally, VIC (MLT of ~0.8 hr) and PIN at MLAT around the brightening onset observed a time delay of the H-component enhancement, supporting the eastward expansion of the auroral brightening (see Figure S1 in Supporting Information S1). These localized signatures are reminiscent of particle injections that could supply power to the ring current.

At middle MLAT, ground magnetometers around midnight in both southern and northern hemispheres observed enhancements in the H component (Figures 2e–2g), indicating current wedges (e.g., Kepko et al., 2014). During the first current wedge, the D-component enhancement at HON in the northern hemisphere (PPT and IPM in the

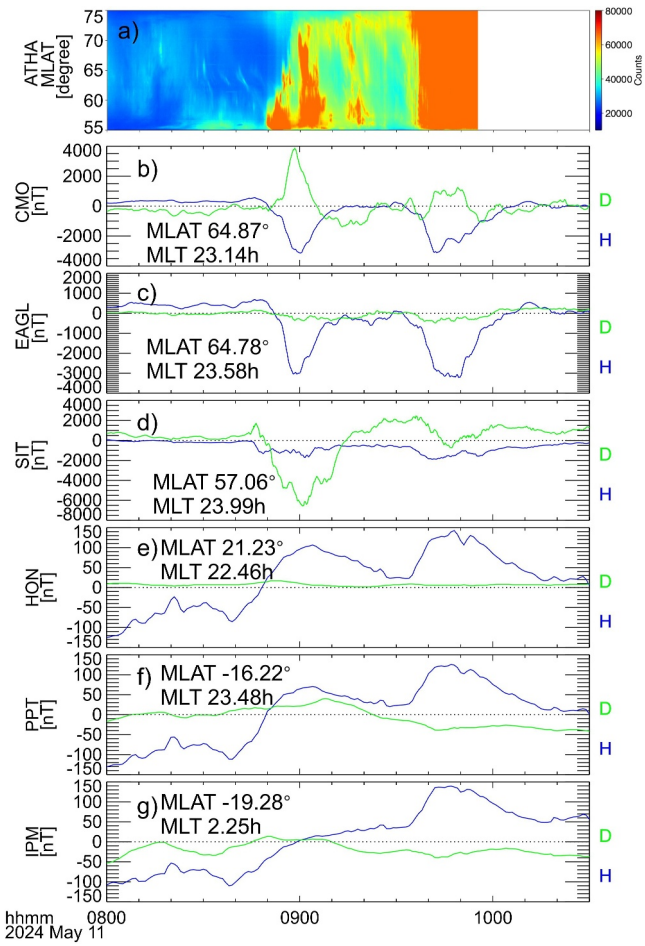

Figure 2. Zoom-in plot to time interval around t5 and t6 for ground observations, including (a) ASI at the ATHA station with 6s cadence, (b)–(d) geomagnetic field disturbances at high-latitude stations from THEMIS GMAG with 1s cadence, and (e)–(g) geomagnetic field disturbances at mid-latitude stations from INTERMAGNET and SuperMAG with 1 min cadence. The MLT at each panel corresponds to 09:00 UT.

southern hemisphere) suggests that the current wedge was east of HON (west of PPT and IPM), that is, centered between HON and PPT (between ~22.5 and 23.5 hr). The identified current wedges suggest that the particle injections were likely associated with DFBs driven by magnetotail reconnection (e.g., Liu et al., 2018).

The vertical TEC map using the 1-s Global Navigation Satellite System (GNSS) receivers in North America (see Movie S4) shows that the first auroral brightening occurred to the west of Seattle. The TEC increased further over Seattle and the enhanced TEC rapidly expanded eastward, consistent with the eastward expansion of the aurora in Movies S2 and S3. The onset MLT was before 0.7 hr, consistent with that the current wedge was centered at the pre-midnight sector, and the onset MLAT was ~53°, consistent with Figure 2a. The onset MLAT was clearly lower than usual (e.g., Gjerloev et al., 2007), suggesting that magnetotail reconnection occurred closer to Earth than typically observed during substorms (~−20 to −30 R_E). To further investigate this, we conduct GOES-18 observations (Figure 3) whose MLT was around the first current wedge (blue in Figure 1j at t5).

Before the first vertical dotted line, GOES-18 observed a B_x enhancement up to ~250 nT relative to the international geomagnetic reference field (IGRF; Figure 3d), indicating a magnetotail-like field geometry at geosynchronous orbit with an extremely thin current sheet (as sketched in Figure 3j). Around the first vertical dotted line, GOES-18 observed dipolarization signatures, as evidenced by an increase in B_z and a decrease in B_x (Figure 3d; relative to IGRF model), accompanied by proton and electron flux enhancements (Figures 3e and 3f), consistent with a DFB. A few minutes later, the dipolarization signatures and particle injections were also observed at GOES-16 (magenta in Figure 1j at t5). Considering the eastward expansion of the auroral brightening, the time lag between GOES-18 and GOES-16 can be explained as eastward expansion of the substorm-like injection. These results support that NERX likely occurred close enough for the resultant DFB in the reconnection outflow to penetrate geosynchronous orbit over a wide range of MLT to supply power to the ring current at that time (It was not declared to be a VNERX because aside from the lack of equatorial spacecraft, magnetic field mapping is not accurate enough to specify the equatorial footpoint of the ionospheric activation and hence of the inferred X-line location).

Next, we discuss what might drive this NERX activity. Figure 3a shows that there was a dynamic pressure pulse around 5 min before the maximum B_x at GOES-18 (Figure 3d). The 5-min delay is consistent with the propagation time from TH-C (X ~ 41 R_E, solar wind speed ~700–800 km/s). Thus, it was likely the dynamic pressure pulse that strongly compressed the magnetosphere leading to the extremely thin current sheet at GOES-18 (sketched in Figure 3j). As upstream dynamic pressure suddenly decreased, the thin current sheet became destabilized, potentially triggering reconnection.

Later, the substorm-like signatures reached their recovery phase while the upstream dynamic pressure was rather stable. At ~09:30 UT, the upstream dynamic pressure started to increase significantly (Figure 3a). Around 5 min later at the second vertical dotted line, GOES-18 observed that B_x started to increase and B_z started to decrease suggesting another current sheet thinning (Figure 3d), while the field strength at GOES-16 started to increase (Figure 3g), due to global compression. Probably because magnetotail reconnection occurred immediately after the current sheet thinning, B_z at GOES-18 increased against the global compression (Figure 3d) accompanied by particle injections (Figures 3e and 3f), the second current wedge (Figures 2e–2g or Figure 3c), intense auroral brightening (Figure 2a), and significant ionospheric current (Figures 2b–2d or Figure 3b). These results suggest that another NERX event likely occurred close enough to cause a DFB to reach geosynchronous orbit and contribute to the ring current again.

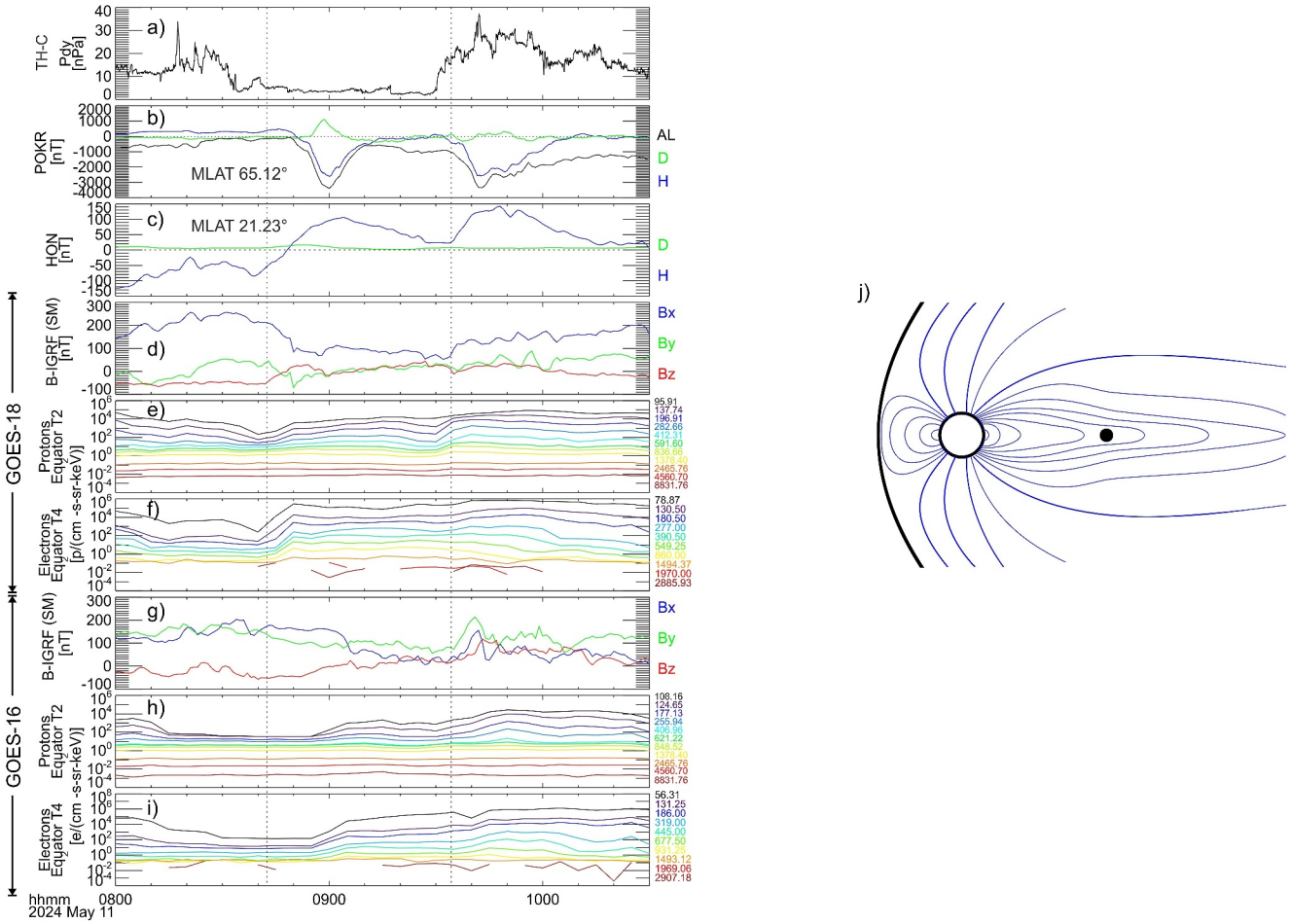

Figure 3. Zoom-in plot to time interval around t5 and t6 for geosynchronous observations, including (a) TH-C observations of dynamic pressure, geomagnetic field disturbances by (b) POKR station and (c) HON station, GOES-18 observations of (d) magnetic field variation relative to IGRF model, (e) proton flux (with energies of each channel in keV on the right), and (f) electron flux, GOES-16 observations of (g) magnetic field variation relative to IGRF model, (h) proton flux, and (i) electron flux, and (j) a simple sketch illustrating a strongly compressed magnetosphere so that GOES-18 (black dot) at the geosynchronous orbit observed magnetotail-like field geometry with current sheet thinning (blue lines). Vertical dotted lines indicate the start of DFBs.

4. Summary

During the recovery phase of the major geomagnetic storm in May 2024, we identified that near-Earth reconnection could occur close enough for DFBs to penetrate geosynchronous orbit to contribute to the ring current: (a) Intense auroral brightening and strong ionospheric currents were observed around midnight, indicative of particle injections. (b) The current wedges identified by mid-MLAT ground magnetometers around midnight indicate that the particle injections could be associated with DFBs, suggesting magnetotail reconnection. (c) The MLAT of the auroral brightening onset was very low indicating that the magnetotail reconnection likely occurred closer to Earth than typically observed during substorms. (d) GOES-18 around midnight detected DFB signatures following an extremely thin (magnetotail-like) current sheet. The driver of this process was likely the large upstream dynamic pressure that strongly compressed the magnetosphere leading to the extremely thin current sheet at geosynchronous orbit. Such upstream conditions are common during the CME suggesting that NERX might contribute to supplying power to the ring current and slowing down its decay during the recovery phase more frequently and efficiently than previously thought. Previous studies have suggested (e.g., Henderson, 2004; Skoug et al., 2003) and demonstrated (Angelopoulos et al., 2020; Beyene & Angelopoulos, 2024) that VNERX can contribute to the ring current during the main phase, yet there were no such observations linking the ring current and magnetotail signatures during the recovery phase. Our study provides further evidence from ground-based observations and the near-Earth magnetotail that NERX likely plays a significant role during storm-time recovery as well.

In this study, the very intense signatures (e.g., AE more than 3,000 nT) made it relatively straightforward to identify the possible NERX events and their upstream drivers. At other times, although there could be similar NERX events that contribute to the storm, their signatures may be difficult to detect because multiple events could overlap each other embedded within background storm perturbations. For example, if the two NERX events in this study were closer to each other, it would have been very difficult to identify them separately. In the future, a statistical study could be conducted using historical and future data from multiple distances (8–15 R_E, such as THEMIS on the nightside) in conjunction with geosynchronous observations and ground observations to determine the occurrence rate of NERX contributing to the ring current during the recovery phase.

Although the observed ground and near-Earth magnetotail signatures were very similar to those of substorms, we avoid calling them substorms but only borrow the lessons learned from how NERX phenomena progress during substorms to apply them to storm times. Principally this is because the substorm growth phase associated with energy loading and storage is absent during storms, or at least it is unrecognizable during storms due to numerous intense activations at multiple local times and latitudes which prevent a secession of AE and subsequent gradual AE increase, the hallmark of growth phase, ahead of the AE intensification related to the injection.

Data Availability Statement

THEMIS (including ARTEMIS, GMAG, and ASI) is available at https://themis.ssl.berkeley.edu/data_retrieval.shtml. KOMPSAT magnetic field data is available at https://swe.ssa.esa.int/sosmag. GOES data is available at https://www.ncei.noaa.gov/data/goes-space-environment-monitor/access/science/. Ground magnetometer data processed using the SuperMAG method is available at https://supermag.jhuapl.edu/mag/?fidelity=low&start=2024-05-11T08%3A00%3A00.000Z&interval=04%3A00&tab=customdownload. Ground magnetometer data in the INTERMAGNET format is available at https://imag-data.bgs.ac.uk/GIN_V1/GINForms2. The SPEDAS software (see Angelopoulos et al. (2019)) is available at https://themis.ssl.berkeley.edu/software.shtml. The TREx ASI data were obtained from https://data.phys.ucalgary.ca/sort_by_project/TREx/RGB/. The GNSS receiver data are available at https://gage-data.earthscope.org/archive/gnss/rinex/obs.

Acknowledgments
TL is partially supported by NASA Grant 80NSSC23K0086. TL and MH acknowledge NASA LWS 80NSSC23K0903. The work of YN was supported by NASA Grants 80NSSC20K0725, 80NSSC21K1321, 80NSSC22K0323, 80NSSC22K0749, 80NSSC23M0193 and 80NSSC23K0410, NSF Grants AGS-1907698 and AGS-2100975, and AFOSR Grants FA9550-23-1-0614 and FA9550-23-1-0634. XS was supported by NASA Grants 80NSSC19K0907, 80NSSC21K1677, and 80NSSC21K1683. MH was partially supported by NASA Grant 80NSSC19K0907. We acknowledge support by the NASA THEMIS contract NAS5-02099. We thank K. H. Glassmeier, U. Auster and W. Baumjohann for the use of the THEMIS/FGM data provided under the lead of the Technical University of Braunschweig and with financial support through the German Ministry for Economy and Technology and the German Center for Aviation and Space (DLR) under contract 50 OC 0302. We also thank the late C. W. Carlson and J. P. McFadden for use of THEMIS/ESA data. We also thank the SPEDAS team and the NASA Coordinated Data Analysis Web. We gratefully acknowledge the SuperMAG collaborators (https://supermag.jhuapl.edu/info/?page=acknowledgement). We also gratefully acknowledge the INTERMAGNET—British Geological Survey. The ASIs are supported by Canada Foundation for Innovation. We gratefully acknowledge the NSF GAGE Data Server for TEC data.

References

Angelopoulos, V. (2008). The THEMIS mission. *Space Science Reviews*, *141*(1), 5–34. https://doi.org/10.1007/s11214-008-9336-1

Angelopoulos, V., Artemyev, A., Phan, T. D., & Miyashita, Y. (2020). Near-Earth magnetotail reconnection powers space storms. *Nature Physics*, *16*(3), 317–321. https://doi.org/10.1038/s41567-019-0749-4

Angelopoulos, V., Baumjohann, W., Kennel, C. F., Coroniti, F. V., Kivelson, M. G., Pellat, R., et al. (1992). Bursty bulk flows in the inner central plasma sheet. *Journal of Geophysical Research*, *97*(A4), 4027–4039. https://doi.org/10.1029/91JA02701

Angelopoulos, V., Cruce, P., Drozdov, A., Grimes, E. W., Hatzigeorgiu, N., King, D. A., et al. (2019). The space physics environment data analysis system (SPEDAS) [Software]. *Space Science Reviews*, *215*(1), 9. https://doi.org/10.1007/s11214-018-0576-4

Angelopoulos, V., Kennel, C. F., Coroniti, F. V., Pellat, R., Kivelson, M. G., Walker, R. J., et al. (1994). Statistical characteristics of bursty bulk flow events. *Journal of Geophysical Research*, *99*(A11), 21257–21280. https://doi.org/10.1029/94JA01263

Angelopoulos, V., McFadden, J. P., Larson, D., Carlson, C. W., Mende, S. B., Frey, H., et al. (2008). Tail reconnection triggering substorm onset. *Science*, *321*(5891), 931–935. https://doi.org/10.1126/science.1160495

Beyene, F., & Angelopoulos, V. (2024). Storm-time very-near-Earth magnetotail reconnection: A statistical perspective. *Journal of Geophysical Research: Space Physics*, *129*(5), e2024JA032434. https://doi.org/10.1029/2024JA032434

Buzulukova, N., Fok, M.-C., Glocer, A., Komar, C., Kang, S.-B., Martin, S., et al. (2018). Geomagnetic storms: First-principles models for extreme geospace environment. In *Extreme events in geospace*. Elsevier. https://doi.org/10.1016/b978-0-12-812700-1.00010-8

Cramer, W. D., Raeder, J., Toffoletto, F. R., Gilson, M., & Hu, B. (2017). Plasma sheet injections into the inner magnetosphere: Two-way coupled OpenGGCM-RCM model results. *Journal of Geophysical Research: Space Physics*, *122*(5), 5077–5091. https://doi.org/10.1002/2017JA024104

Donovan, E., Mende, S., Jackel, B., Frey, H., Syrjäsuo, M., Voronkov, I., et al. (2006). The THEMIS all-sky imaging array—System design and initial results from the prototype imager. *Journal of Atmospheric and Solar-Terrestrial Physics*, *68*(13), 1472–1487. https://doi.org/10.1016/j.jastp.2005.03.027

Dubyagin, S., Sergeev, V., Apatenkov, S., Angelopoulos, V., Runov, A., Nakamura, R., et al. (2011). Can flow bursts penetrate into the inner magnetosphere? *Geophysical Research Letters*, *38*(8), L08102. https://doi.org/10.1029/2011gl047016

Dungey, J. W. (1961). Interplanetary magnetic field and the auroral zones. *Physical Review Letters*, *6*(2), 47–48. https://doi.org/10.1103/physrevlett.6.47

Gjerloev, J. W. (2012). The supermag data processing technique. *Journal of Geophysical Research*, *117*(A9). https://doi.org/10.1029/2012JA017683

Gjerloev, J. W., Hoffman, R. A., Sigwarth, J. B., & Frank, L. A. (2007). Statistical description of the bulge-type auroral substorm in the far ultraviolet. *Journal of Geophysical Research*, *112*(A7), A07213. https://doi.org/10.1029/2006JA012189

Gonzalez, W. D., Joselyn, J. A., Kamide, Y., Kroehl, H. W., Rostoker, G., Tsurutani, B. T., & Vasyliunas, V. M. (1994). What is a geomagnetic storm? *Journal of Geophysical Research*, *99*(A4), 5771–5792. https://doi.org/10.1029/93JA02867

Gonzalez, W. D., Tsurutani, B. T., Gonzalez, A. L. C., Smith, E. J., Tang, F., & Akasofu, S. (1989). Solar wind–magnetosphere coupling during intense magnetic storms (1978–1979). *Journal of Geophysical Research*, *94*(A7), 8835–8851. https://doi.org/10.1029/ja094ia07p08835

Goodman, S. J., Gurka, J., DeMaria, M., Schmit, T. J., Mostek, A., Jedlovec, G., et al. (2012). The GOES-R Proving Ground: Accelerating user readiness for the next-generation geostationary environmental satellite system. *Bulletin of the American Meteorological Society*, *93*(7), 1029–1040. https://doi.org/10.1175/bams-d-11-00175.1

Henderson, M. G. (2004). The May 2–3, 1986 CDAW-9C interval: A sawtooth event. *Geophysical Research Letters*, *31*(11), L11804. https://doi.org/10.1029/2004GL019941

Hofmann-Wellenhof, B., Lichtenegger, H., & Collins, J. (1998). GPS—Global positioning system. In *Theory and practice*. Springer.

Keika, K., Kistler, L. M., & Brandt, P. C. (2013). Energization of O^+ ions in the Earth's inner magnetosphere and the effects on ring current buildup: A review of previous observations and possible mechanisms. *Journal of Geophysical Research: Space Physics*, *118*(7), 4441–4464. https://doi.org/10.1002/jgra.50371

Kepko, L., McPherron, R. L., Amm, O., Apatenkov, S., Baumjohann, W., Birn, J., et al. (2014). Substorm current wedge revisited. *Space Science Reviews*, *190*(1–4), 1–46. https://doi.org/10.1007/s11214-014-0124-9

Kerridge, D. J. (2001). INTERMAGNET: Worldwide near-real-time geomagnetic observatory data. In *European Space Agency Space Weather Workshop*. European Space Research and Technology Centre. Retrieved from www.intermagnet.org/publications/IM_ESTEC.pdf

Kim, B. K. (1999). An overview of the Korea multi-purpose satellite (KOMPSAT). In F.-B. Hsiao (Ed.), *Microsatellites as research tools* (Vol. 10, pp. 66–73). Pergamon. https://doi.org/10.1016/S0964-2749(99)80010-9

Liu, J., Angelopoulos, V., Yao, Z., Chu, X., Zhou, X.-Z., & Runov, A. (2018). The current system of dipolarizing flux bundles and their role as wedgelets in the substorm current wedge. In A. Keiling, O. Marghitu, & M. Wheatland (Eds.), *Electric currents in geospace and beyond*. https://doi.org/10.1002/9781119324522.ch19

MacAlester, M. H., & Murtagh, W. (2014). Extreme space weather impact: An emergency management perspective. *Space Weather*, *12*(8), 530–537. https://doi.org/10.1002/2014SW001095

Magnes, W., Hillenmaier, O., Auster, H. U., Brown, P., Kraft, S., Seon, J., et al. (2020). Space weather magnetometer aboard GEO-KOMPSAT-2A. *Space Science Reviews*, *216*(8), 119. https://doi.org/10.1007/s11214-020-00742-2

Pellat, R., Coroniti, F. V., & Pritchett, P. L. (1991). Does ion tearing exist? *Geophysical Research Letters*, *18*(2), 143–146. https://doi.org/10.1029/91gl00123

Runov, A., Angelopoulos, V., Henderson, M. G., Gabrielse, C., & Artemyev, A. (2021). Magnetotail dipolarizations and ion flux variations during the main phase of magnetic storms. *Journal of Geophysical Research: Space Physics*, *126*(5), e2020JA028470. https://doi.org/10.1029/2020JA028470

Runov, A., Angelopoulos, V., Weygand, J. M., Artemyev, A. V., Beyene, F., Sergeev, V., et al. (2022). Thin current sheet formation and reconnection at $X \sim -10$ RE during the main phase of a magnetic storm. *Journal of Geophysical Research: Space Physics*, *127*(9), e2022JA030669. https://doi.org/10.1029/2022JA030669

Russell, C. T., Chi, P. J., Dearborn, D. J., Ge, Y. S., Kuo-Tiong, B., Means, J. D., et al. (2009). THEMIS ground-based magnetometers. In J. L. Burch & V. Angelopoulos (Eds.), *The THEMIS mission*. Springer. https://doi.org/10.1007/978-0-387-89820-9_17

Sciola, A., Merkin, V. G., Sorathia, K., Gkioulidou, M., Bao, S., Toffoletto, F., et al. (2023). The contribution of plasma sheet bubbles to stormtime ring current buildup and evolution of its energy composition. *Journal of Geophysical Research: Space Physics*, *128*(11), e2023JA031693. https://doi.org/10.1029/2023JA031693

Sergeev, V. A., Chernyaev, I. A., Dubyagin, S. V., Miyashita, Y., Angelopoulos, V., Boakes, P. D., et al. (2012). Energetic particle injections to geostationary orbit: Relationship to flow bursts and magnetospheric state. *Journal of Geophysical Research*, *117*(A10), A10207. https://doi.org/10.1029/2012JA017773

Skoug, R. M., Thomsen, M. F., Henderson, M. G., Funsten, H. O., Reeves, G. D., Pollock, C. J., et al. (2003). Tail-dominated storm main phase: 31 March 2001. *Journal of Geophysical Research*, *108*(A6), 1259. https://doi.org/10.1029/2002JA009705

Sorathia, K. A., Michael, A., Merkin, V. G., Ukhorskiy, A. Y., Turner, D. L., Lyon, J. G., et al. (2021). The role of mesoscale plasma sheet dynamics in ring current formation. *Frontiers in Astronomy and Space Sciences*, *8*. https://doi.org/10.3389/fspas.2021.761875

Yang, J., Toffoletto, F. R., & Wolf, R. A. (2016). Comparison study of ring current simulations with and without bubble injections. *Journal of Geophysical Research: Space Physics*, *121*(1), 374–379. https://doi.org/10.1002/2015JA021901

Yang, J., Toffoletto, F. R., Wolf, R. A., Sazykin, S., Ontiveros, P. A., & Weygand, J. M. (2012). Large-scale current systems and ground magnetic disturbance during deep substorm injections. *Journal of Geophysical Research*, *117*(A4), A04223. https://doi.org/10.1029/2011JA017415